Supplementary Figures

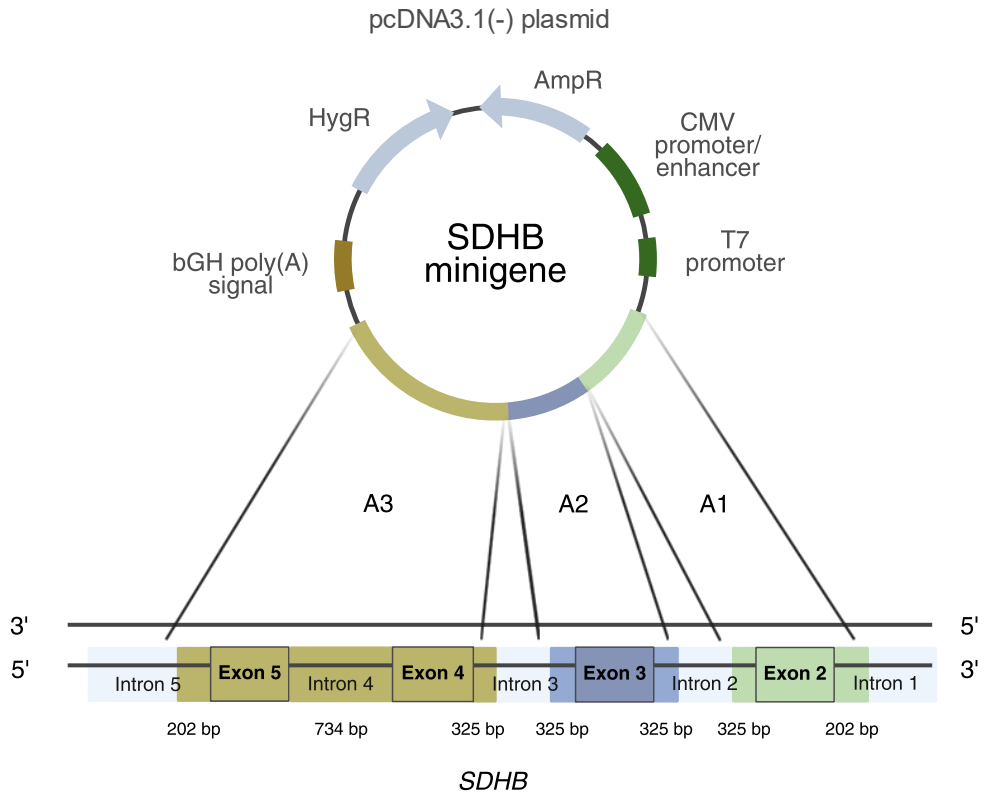

Supplemental Figure 1. Schematic representation of SDHB minigene with exon 2 to 5. (Created in BioRender. Köhler, A. (2026))

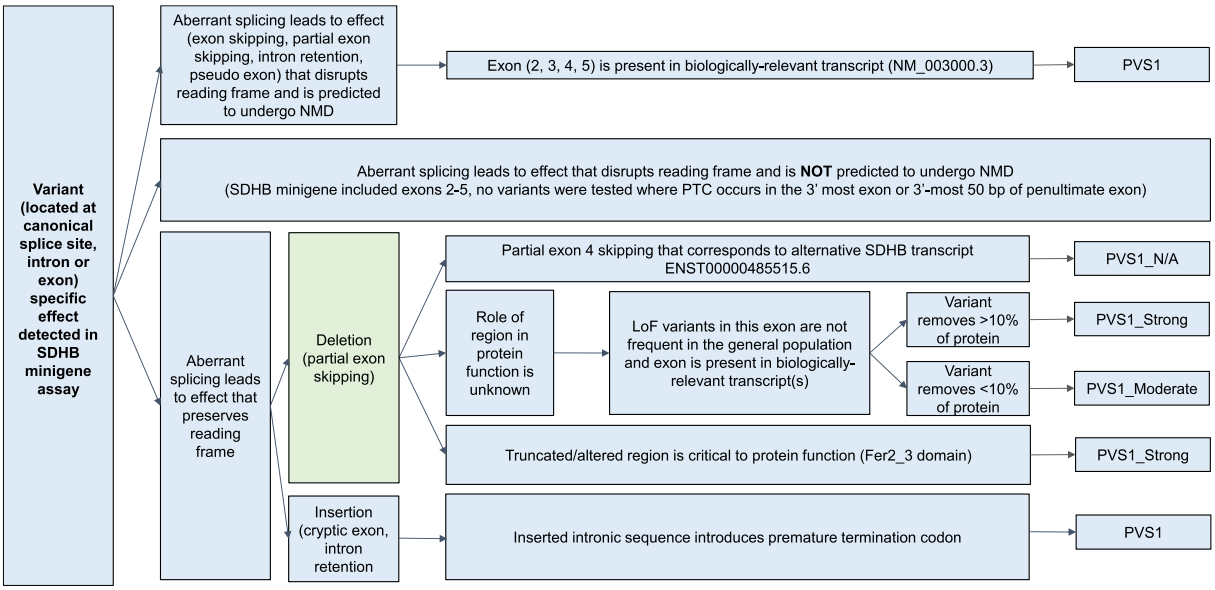

Supplemental Figure 2a. PVS1 decision tree (Abou Tayoun et al., 2018) adapted to SDHB minigene

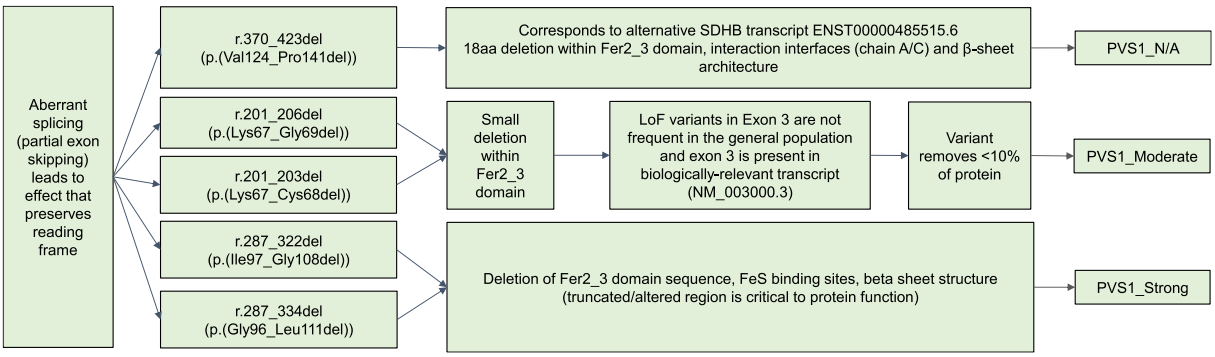

Supplemental Figure 2b. PVS1 decision tree for in-frame transcripts observed in SDHB minigene assay

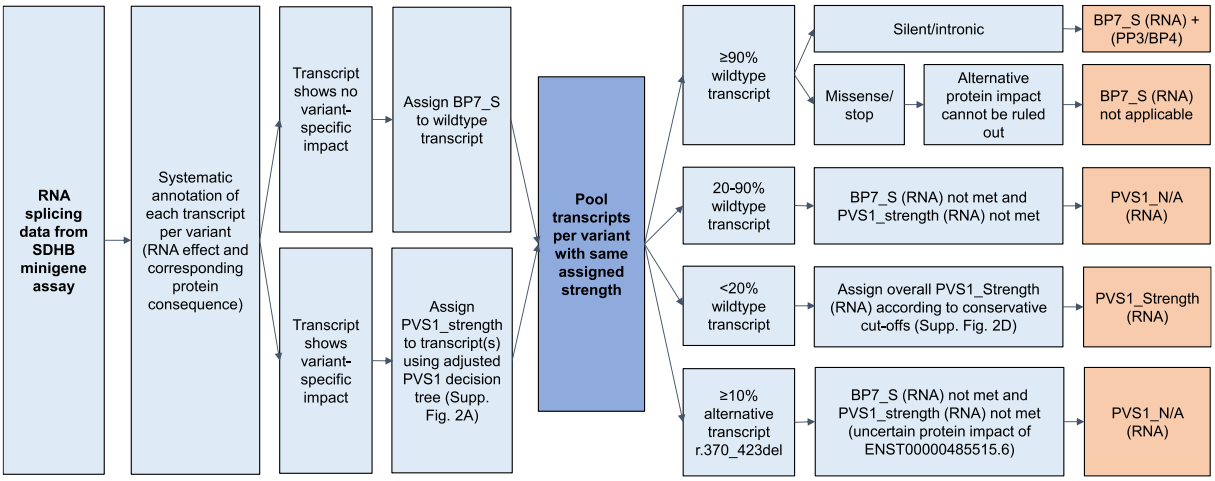

Supplemental Figure 2c. Decision tree for overall ACMG classification of RNA data derived from SDHB minigene

Proportion of pooled aberrant transcripts produced by variant allele	Overall PVS1_Strength (RNA)
≥90% PVS1	PVS1_Strong (RNA)
≥90% PVS1_Strong or 80-90% PVS1	PVS1_Moderate (RNA)
≥90% PVS1_Moderate or ≥90% PVS1_Supporting or 80-90% PVS1_Strong / _Moderate / _Supporting	PVS1_Supporting (RNA)
If multiple PVS1_strength categories are present within one variant, the overall strength is assigned according to the lowest category	

Supplemental Figure 2d. Table with conservative cut offs for pooled aberrant transcripts (Parsons et al., 2024)

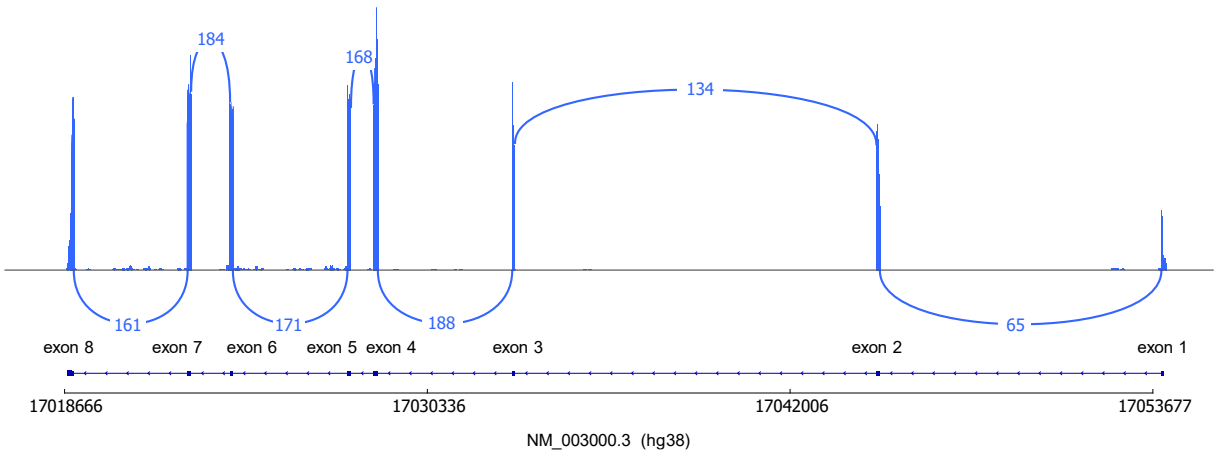

Supplemental Figure 3. RNA-Seq data of endogenous SDHB in HEK293T visualized as sashimi plot (Created in IGV)

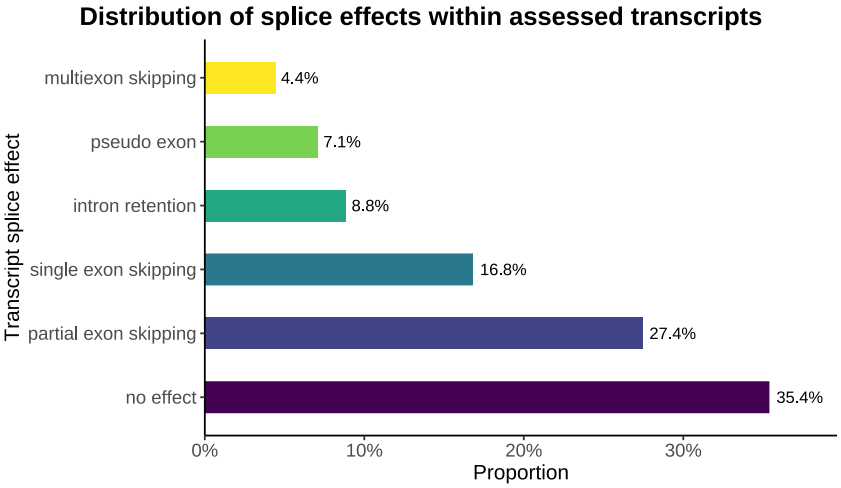

Supplemental Figure 4. Bar chart showing distribution of splice effects in analyzed transcripts (n = 113) (created with R)

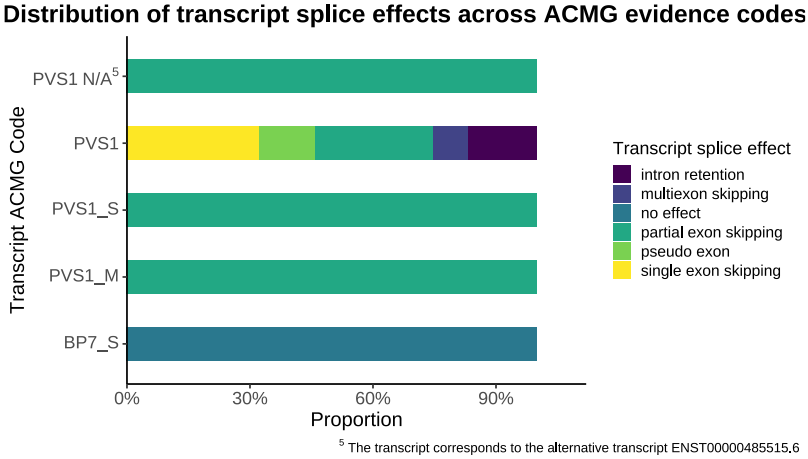

Supplemental Figure 5. Bar chart showing observed splice effects per assigned ACMG codes in all assessed transcripts (n=113) (created with R)

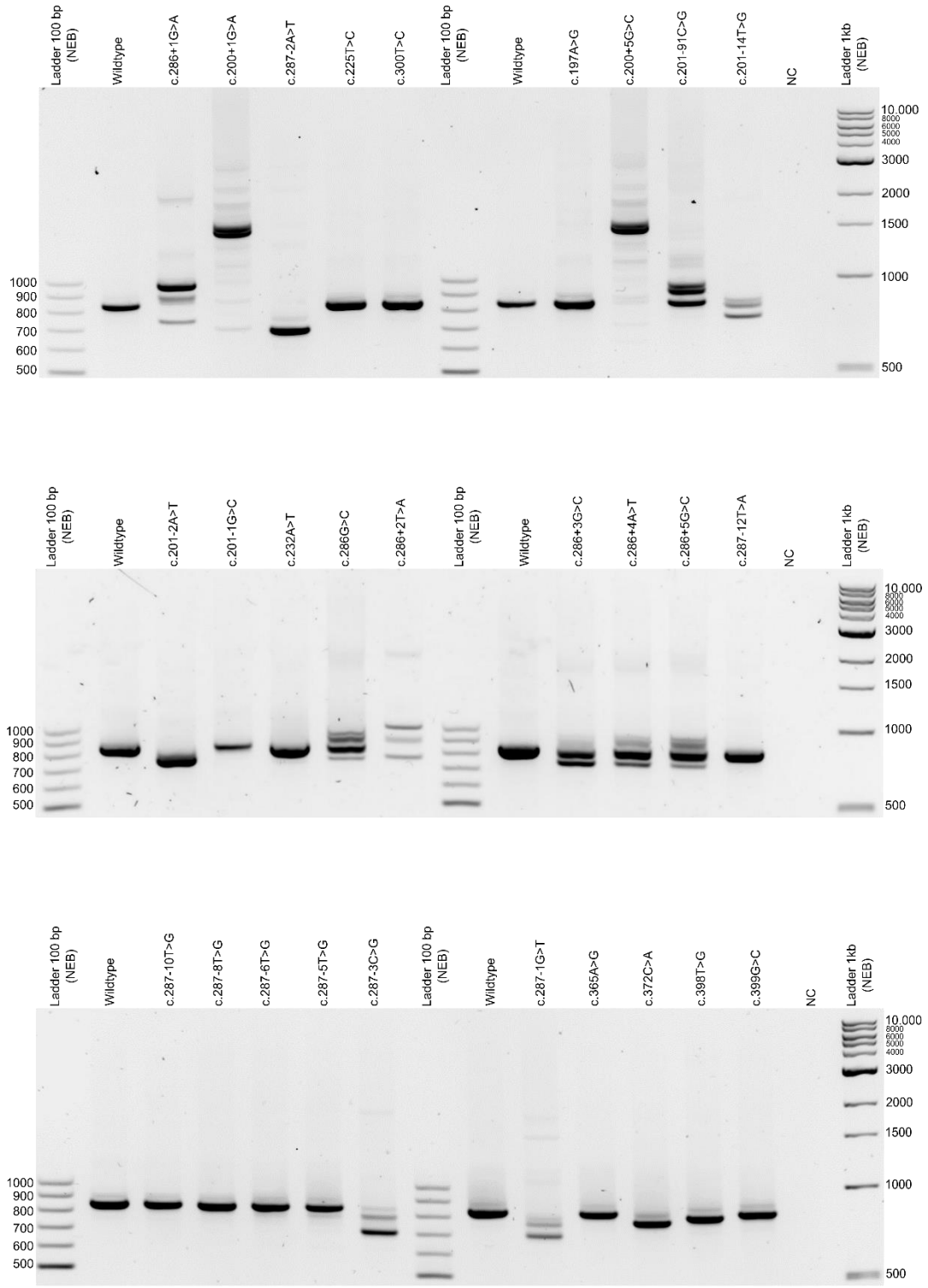

Supplemental Figure 6a. Results from gel-electrophoresis of RT-PCR products, run at 110V for 1h 15min. in 1% agarose gel

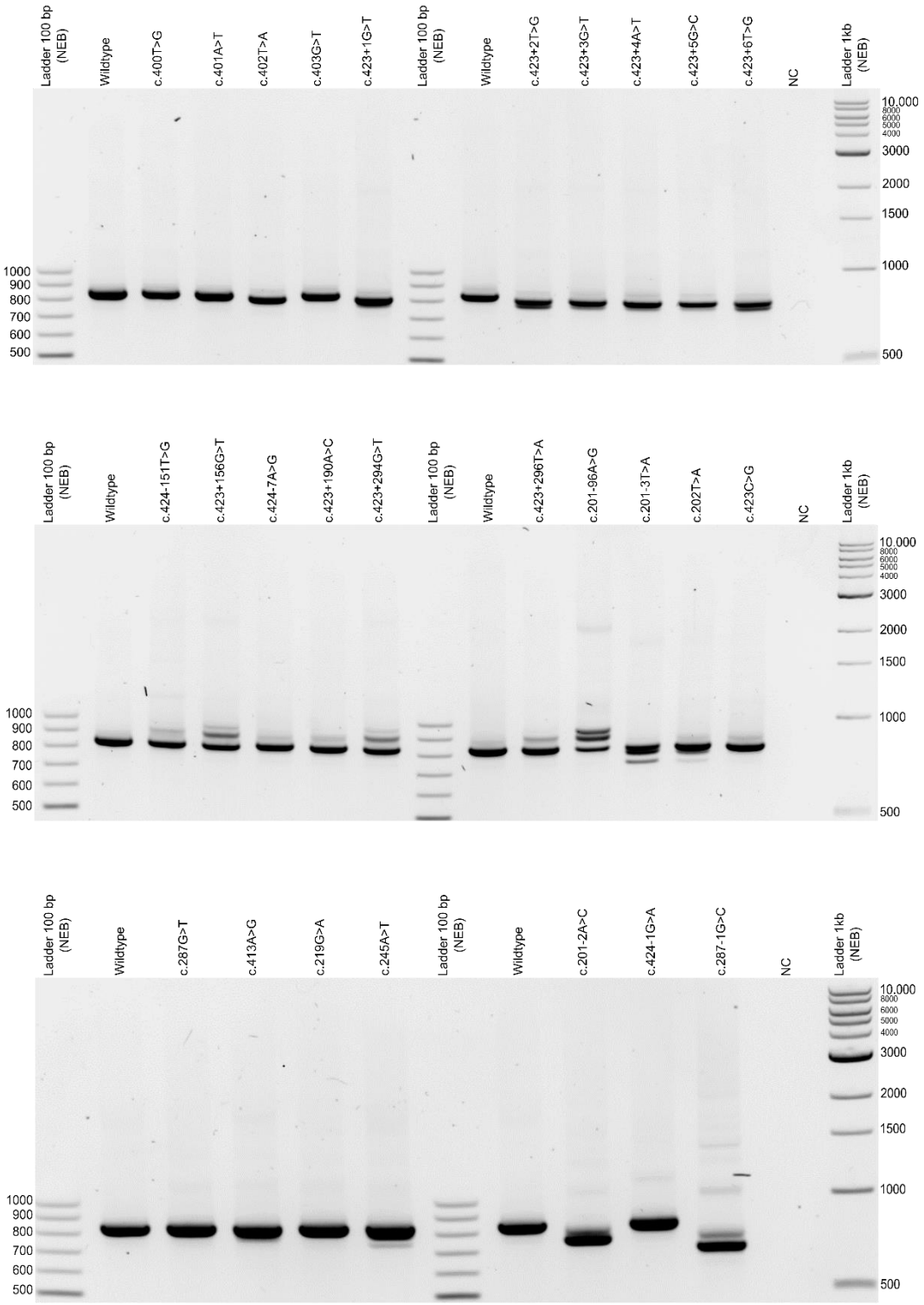

Supplemental Figure 6b Results from gel-electrophoresis of RT-PCR products, run at 110V for 1h 15min. in 1% agarose gel

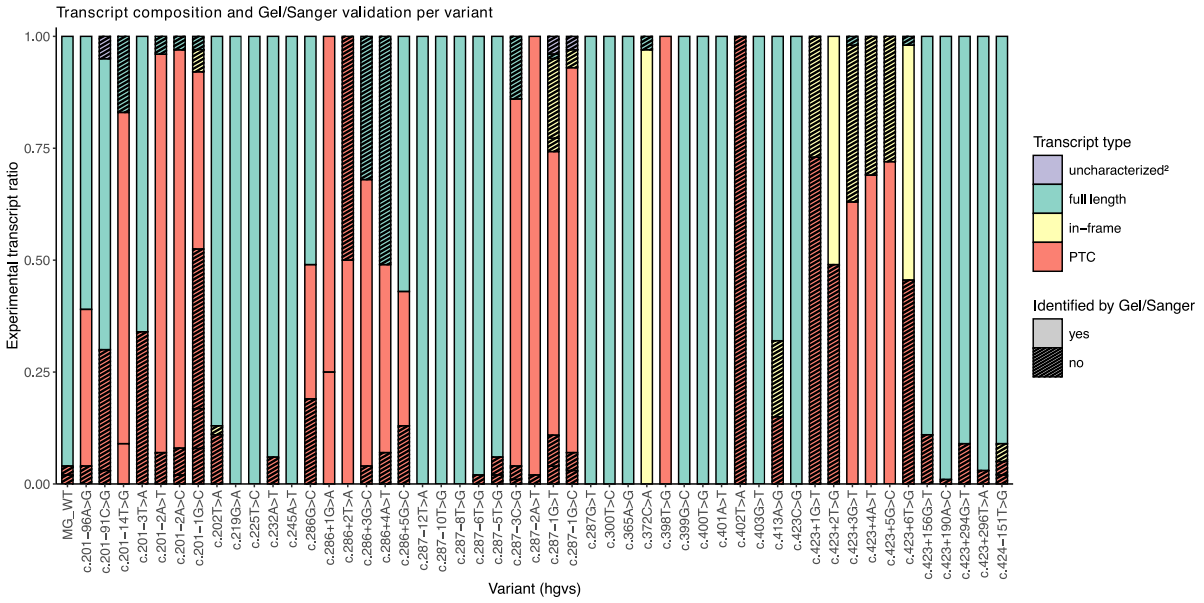

Supplemental Figure 7. Bar chart representing the distribution of transcript types observed in transcriptional analysis annotated with proportion of transcripts that could not be identified by Gel/Sanger method (created with R)

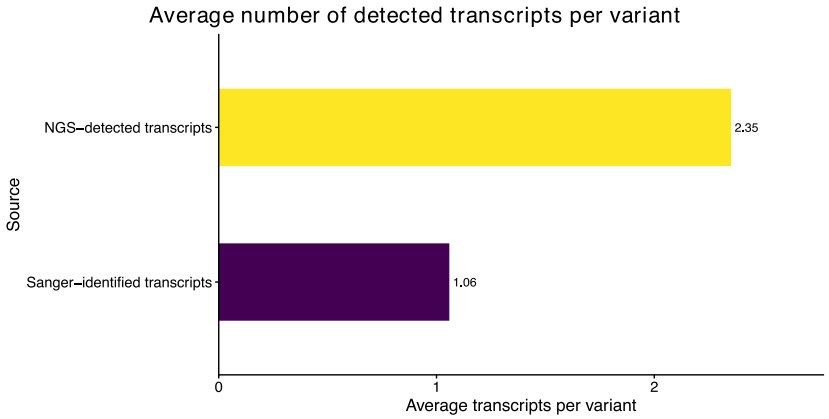

Supplemental Figure 8. Bar chart showing difference in resolution of transcript number comparing NGS approach with conventional Gel/sanger method (created with R)